ELSEVIER

Ceramics International 33 (2007) 589–593

CERAMICS INTERNATIONAL

www.elsevier.com/locate/ceramint

# Mean dopant ion radius dependency of electrical resistivity in the $Zn_{1-x-y}Ga_xIn_yO$ system

Katsuyoshi Kakinuma *, Takahiro Shiho, Misachi Watanabe, Hiroshi Yamamura

*Department of Applied Chemistry, Faculty of Engineering, Kanagawa University, 3-27-1 Rokkakubashi, Kanagawa-ku, Yokohama 221-8686, Japan*

Received 2 November 2005; received in revised form 16 November 2005; accepted 29 November 2005
Available online 15 February 2006

**Abstract**

The electrical resistivity of the $Zn_{1-x-y}Ga_xIn_yO$ system was investigated as a function of the dopant content and mean dopant ion radius. The electrical resistivity of all members of the system exhibited metallic behavior as a function of temperature. The lowest electrical resistivity at 873 K fell to $2.81 \times 10^{-3}$ (Ω cm) in $Zn_{0.99}Ga_{0.0073}In_{0.0027}O$. In cases with the same dopant content, the resistivity strongly depended on the mean dopant ion radius, but the Seebeck coefficient was unrelated to those radii. Regardless of dopant content, the minimum resistivity of this system appeared around a mean dopant ion radius of 0.54 Å. Evidently, the carrier mobility is strongly dependent on the magnitude of the mean dopant ion radius and any structural distortion.


*Keywords:* B. Defect; C. Electrical property; D. ZnO

## 1. Introduction

Transparent electrode materials have a high transparency in the visible light coupled with low electrical resistivity. Representatives of such materials include $In_2O_3$ and ZnO, which are used as electrodes in liquid-crystal displays and in solar cells. Zinc oxide is a wide-gap semiconductor, with a wurzite structure. The electrical resistivities of the ZnO-$ZrO_2$, [1] ZnO-$Al_2O_3$, [2] and ZnO-$In_2O_3$-$SnO_2$ systems [3] are lower than that of undoped ZnO; in addition, they show good transparency in the visible region. This type of system has a conduction band and valence band, both constructed from the $sp^3$ hybrid orbitals of the Zn4s and O2p [4,5]. The band gap energy is 3.3 eV, which is too large to allow visible light to excite an electron from the valence to the conduction band. Impurities of Vo'', $Zn_i^{\bullet}$ or $Zn_i^{\bullet\bullet}$ types act as low level donors, and affect electrical resistivity behavior without changing the transparency in the visible region [5,6].

In order to precisely elucidate the conducting mechanism of the doped ZnO system, we have measured the Hall coefficient and electrical resistivity, thus allowing us to estimate the carrier density and mobility. In the case of the heavily impurity-doped ZnO system, the carrier scattering of the ionized impurity was reported to dominate the carrier mobility [7–9]. We have determined that the electrical conductivity of the ZnO system, doped to the same content of aliovalent cation, was strongly dependent on the mean dopant ion radius, and that the Ga and In-doped ZnO system displays the lowest electrical resistivity among the many kinds of co-doped ZnO systems [10].

In the present paper, we focus on the Ga and In co-doped ZnO system, through an investigation of the electrical resistivity and Seebeck coefficient as a function of three variables: the total dopant ion content, the temperature, and the mean dopant ion radius. We then determine the dominant parameter involved in the electrical resistivity.

## 2. Experimental details

Powder samples of the ZnO system compounds were prepared by a solid-state reaction. The starting materials i.e. ZnO (99.999%, High Purity Chemical Co., Ltd.), $In_2O_3$

* Corresponding author. Tel.: +81 45 481 5661x3878; fax: +81 45 413 9770.
*E-mail address:* kakink01@kanagawa-u.ac.jp (K. Kakinuma).

0272-8842/$32.00 
doi:10.1016/j.ceramint.2005.11.008

(99.99%, High Purity Chemical Co., Ltd.), and $Ga_2O_3$ (99.99%, High Purity Chemical Co., Ltd.), were mixed for 24 h with a ball mill. The mixture was dried at 373 K for several hours, and then calcined at 1073 K for 5 h. The powder, which was sieved to under 54 μm, was pressed at 50 kgf/cm$^2$ into a rectangular shape (30 mm × 5 mm × 5 mm) and then isostatically pressed again at 2000 kgf/cm$^2$. These samples were sintered at 1673 K for 10 h in air.

The crystal structures of the sintered samples were determined by X-ray diffactometry (Multiflex Rigaku Co., Ltd.) using Cu Kα radiation at room temperature. Their microstructures were observed by scanning electron microscopy (JEOL JSM-5200). Their electrical resistivities were measured by the DC four-probe method from room temperature to 1173 K in dry air. Platinum electrodes were attached to the samples by means of a firing at 1173 K for 1 h in air. To attain an equilibrium state, we measured the high temperature after maintaining the given temperature for several hours. The mean dopant ion radius was calculated by the formula (1):

$$\text{mean dopant ion radius} = r_{\mathrm{M}} \frac{x}{x+y} + r_{\mathrm{M}'} \frac{y}{x+y} \tag{1}$$

where $r_{\mathrm{M}}$ and $r_{\mathrm{M}'}$ are the dopant ion radius, [11] and $x$ and $y$ are the cation stoichiometric composition ratios of the two respective kinds of dopant ions.

## 3. Results and discussion

Except for slight shifts in the diffraction angles and small differences in the breadth of the peaks, the X-ray powder diffraction patterns of the $Zn_{1-x-y}Ga_xIn_yO$ ($0 \leqq x+y \leqq 11 \times 10^{-3}$) system were identical to that of ZnO. The spinel phase of $ZnIn_2O_4$ or $ZnGa_2O_4$ appeared as impurities above the solubility limit. The relative densities of all the sintered specimens, which were estimated from their dimensions and weight, were over 95%. From the SEM photographs, we confirmed that each sample was well sintered and that grain surface streaks did not exist in any of the samples. With increases in the total dopant content, the color of the sintered samples changed from white to light gray.

The donor level of $Zn_i^{\bullet}$ and $Zn_i^{\bullet\bullet}$ in ZnO system appears below the conduction band. The defect reaction is influenced by the annealing temperature and oxygen partial pressure. In some cases, differences in the sintering process generate hysteresis in plots of the electrical resistivity as a function of physical variables [12]. In order to detect that defect reactions had reached equilibrium, we have confirmed precisely the reproducibility of the electrical resistivity and Seebeck coefficient results against temperatures above 773 K.

In Fig. 1, we provide the results of our measurements of Seebeck coefficient ($\alpha$) of the doped ZnO system at 873 K. This system, in which the total dopant content ($x + y$) was $7 \times 10^{-3}$, was selected as a representative one. We found that the coefficient was independent of the mean dopant ion radius, and that, in the ZnO semiconductor, the carrier density follows the

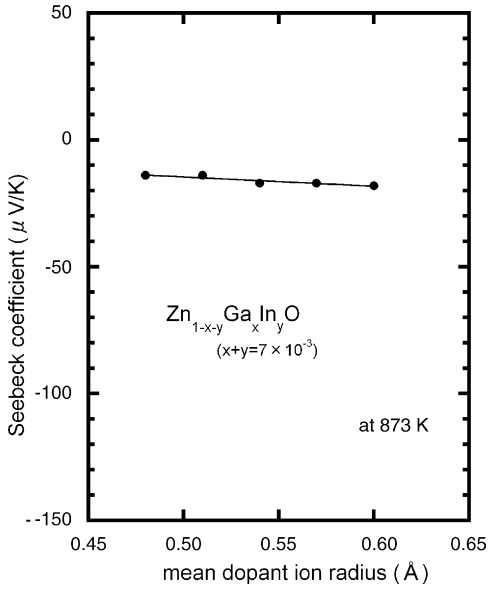


Fig. 1. Seebeck coefficient of the $Zn_{1-x-y}Ga_xAl_yO$ system at 873 K as a function of mean dopant ion radius.

Maxwell-Boltzmann distribution. The Seebeck coefficient obeys the following formula:

$$\alpha = \frac{k}{e}\left\{\ln\left[\frac{N_{\mathrm{c}}(T)}{n}\right] + m\right\} \tag{2}$$

where $k$, $e$, $N_{\mathrm{c}}(T)$, $n$, $m$ are, respectively, the Boltzmann constant, the elementary charge, the density of states for the conduction band, the carrier density, and a constant. This formula indicates that, at constant temperature, the Seebeck coefficient is dependent on the carrier density. Presumably, the fact that the Seebeck coefficient is independent of the mean dopant ion radius would imply that the carrier density remains the same against the ion radius, when the total dopant ion content is kept constant.

In Fig. 2a–e, we provide plots of the resistivity of the ZnO systems as a function of temperature. The electrical resistivity of all the compounds behaved in a metallic fashion. In the metallic region, the resistivity as a function of temperature obeys Matthiessen's law. Here, the resistivity is divided into two parts as follows:

$$\rho = \rho_{\mathrm{th}} + \rho_i \tag{3}$$

the $\rho_{\mathrm{th}}$ part is dependent on the temperature, and is connected by phonons to the carrier scattering, as in:

$$\rho_{\mathrm{th}} = \frac{m\nu_{\mathrm{F}}}{\eta|e|^2}\frac{T}{\alpha} \tag{4}$$

where $m$, $\nu_{\mathrm{F}}$, $\eta$, $e$, $\alpha$, and $T$ are, respectively, the mass and drift velocity of the electron, and the carrier density, elementary electric charge, a proportionality constant, and temperature. The size of $\rho_{\mathrm{th}}$ is related to the thermal vibrations of the atoms in the compound and not to scattering from an impurity or lattice defect. As Fig. 2a–e show, the high temperature resistivities above 773 K paralleled each other, a result suggesting

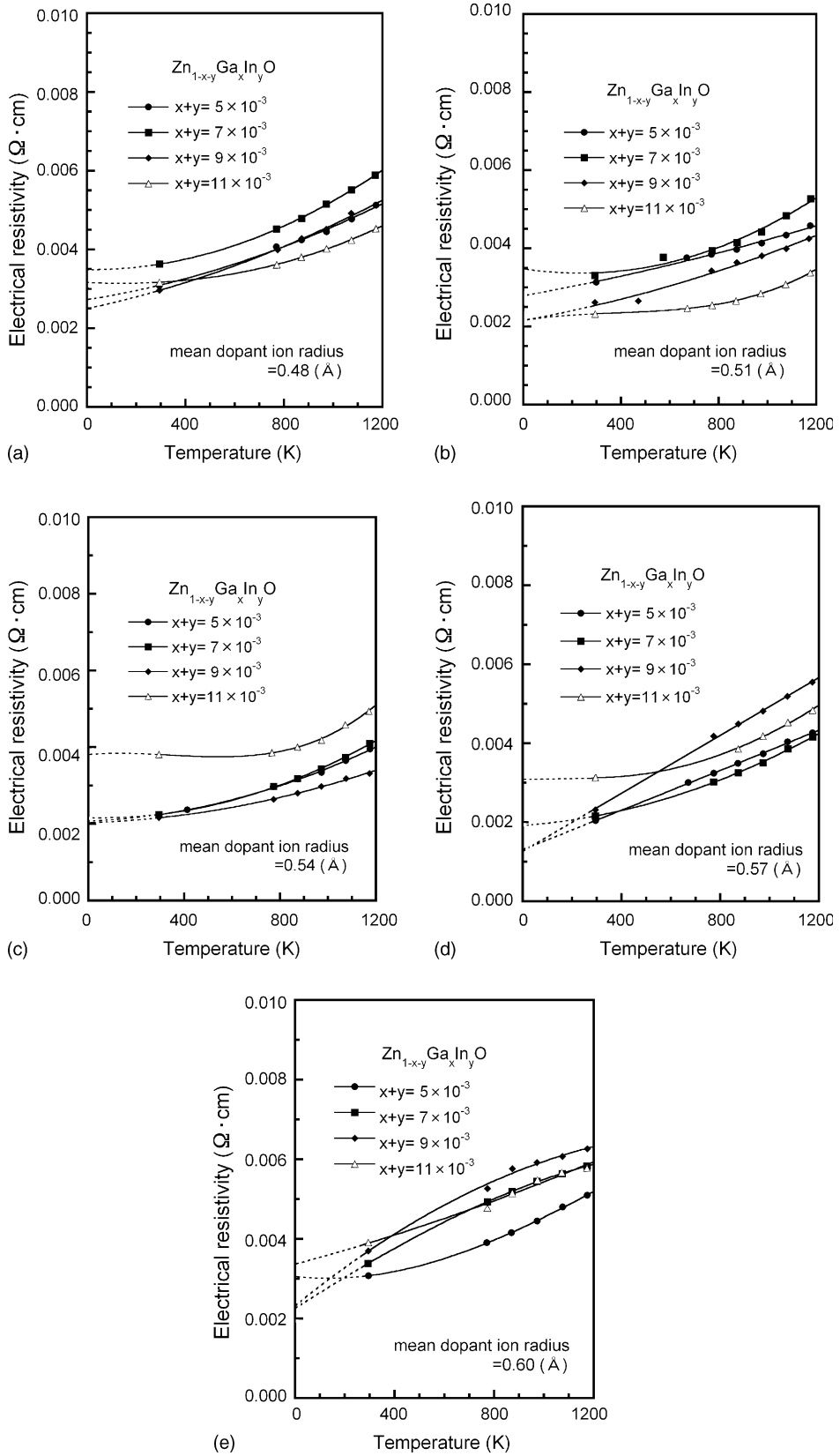


Fig. 2. Electrical resistivity of the $Zn_{1-x-y}Ga_xAl_yO$ system for mean dopant ion radius (Å): (a) 0.48; (b) 0.51; (c) 0.54; and (d) 0.60.

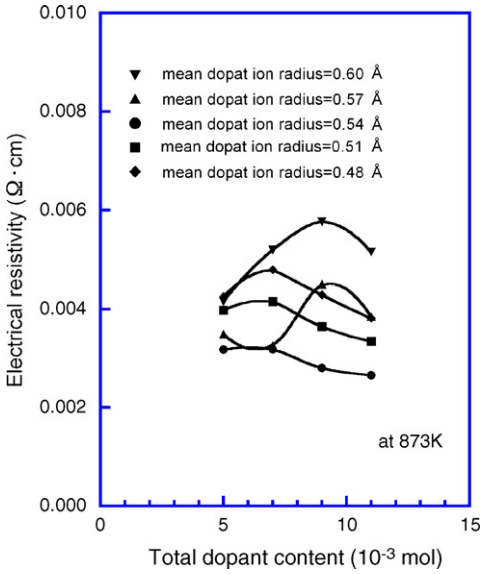


Fig. 3. Electrical resistivity of the $Zn_{1-x-y}Ga_xAl_yO$ system at 873 K as a function of the total dopant content.

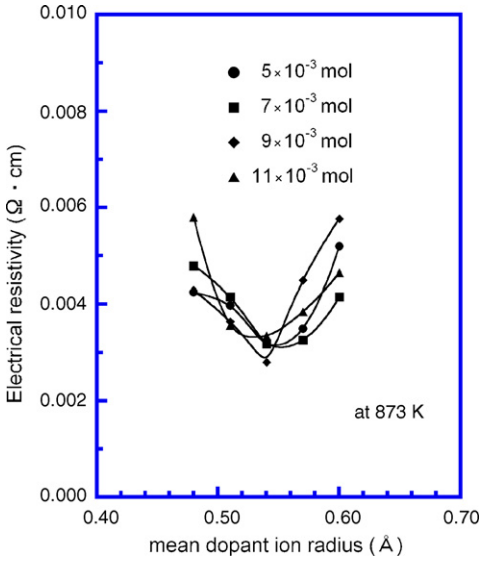


Fig. 4. Electrical resistivity of the $Zn_{1-x-y}Ga_xAl_yO$ system at 873 K as a function of the mean dopant ion radius.

that, at high temperatures, the temperature dependency of the electrical resistivity would mainly arise from thermal vibrations. The other part of the resistivity, $\rho_i$, is defined to be the residual resistivity; it is described as follows:

$$\rho_i = \frac{m v_F}{\eta |e|^2} \left( \frac{x_i}{a} \right) \tag{5}$$

where $x_i$ is the impurity content and $a$ is the distance between Zn and O atoms.

Fig. 3 shows the resistivity at 873 K as a function of the dopant content. Each electrical resistivity exhibited a different dopant content dependency. Since the total dopant content is quite high, we assume that the variation in $1/\alpha$, $x_i$ and $\eta$ with dopant content could be neglected, and that, instead, the value of the velocity $v_F$ would mainly influenced on the electrical resistivity.

The variation in electrical conductivity at 873 K with mean dopant ionic radius at several total dopant content levels are shown in Fig. 4. The electrical resistivity decreased as the mean dopant ion radius became smaller, and fell to a minimum value around the value of 0.54 Å for any dopant content. Above this 0.54 Å value, the electrical resistivity of all of the systems increased. For the same co-dopant content, the carrier density would remain constant, as shown by the Seebeck coefficient results shown in Fig. 1. Evidently, the electrical resistivity behavior illustrated in Fig. 4 is related to the carrier mobility, which is directly connected with the carrier velocity ($v_F$).

The carrier mobility of a metallic oxide is influenced by the impurity scattering. In the case of scattering from a neutral impurity, the mobility is constant with temperature; thus, it would be a negligible factor in the ZnO system. The metallic behavior of this system indicates a carrier concentration of more than $10^{18}$ ($cm^{-3}$) at low dopant levels, [7–9] and most of the dopant cation was ionized. The effect of the ionized impurity scattering diminishes with the decrease in the ion radii of the dopant cation. Minami et al. also reported that the carrier electron was scattered by the ionized dopant in regions with a high content of dopant [13]. Presumably, the ionized impurity would be one of the principal scattering factors when the mean dopant ion radius are between 0.60 and 0.54 Å.

Below a mean dopant ion radius of 0.54 Å, the effect of ionized impurity scattering might well decrease. But, the electrical resistivity increased against mean dopant ion radius. With regard to the crystal chemistry, another report noted that the ion radius ratio between the zinc and oxide ion was above 0.414 [11]. This value of the ratio means that the octahedral structure is a stable form of coordination between Zn and O [14]. But the ZnO system normally forms a tetrahedral structure because of the $sp^3$ hybrid bonding between the Zn4s and the O2p [4,5]. A decrease in the mean dopant ion radius below 0.54 Å would distort the crystal structure. Because this distortion could cause structural defect scattering, it might reduce the velocity of $v_F$.

## 4. Conclusions

In order to elucidate the dominant parameter determining the conductivity in the doped ZnO system, we measured the conductivity of $Zn_{1-x-y}Ga_xIn_yO$ ($0 \leqq x+y \leqq 11 \times 10^{-3}$) samples from room temperature to 1173 K. The conductivity in the equilibrium state was strongly dependent not only on the dopant ion content but also on the dopant ion radius. The minimum resistivity appeared around a mean dopant ion radius of 0.54 Å for all dopant contents. With the same total dopant content, the carrier density remained constant. The relationship between the electrical resistivity and the mean dopant ion radius was influenced by the amount of ionized impurities and structural distortion.

## Acknowledgements

This study was supported by a High Technology Research Project grant at Kanagawa University from the Ministry of Education, Science, Sports and Culture.

## References

[1] S.B. Qadri, H. Kim, H.R. Khan, A. Pique, J.S. Horwitz, D. Chrisey, W.J. Kim, E.F. Skelton, Thin Solid Films 377–378 (2000) 750–754.
[2] K. Tominaga, N. Umezu, I. Mori, T. Ushiro, T. Moriga, I. Nakabayashi, Thin Solid Films 316 (1998) 85–88.
[3] T. Minami, T. Kakumu, K. Shimokawa, S. Tanaka, Thin Solid Films 317 (1998) 318–321.
[4] G. Zwicker, K. Jacobi, Solid State Commun. 54 (1985) 701–704.
[5] V. Gavryushin, G. Raciukaitis, D. Juodzbalis, A. Kazlauskas, V. Kubertavicius, J. Cryst. Growth 138 (1994) 924–933.
[6] P. Bonasewicz, W. Hirschwald, G. Neumann, Phys. Stat. Sol. (a) 97 (1986) 593–599.
[7] T. Minami, S. Tanaka, H. Sato, H. Sonohara, J. Vac. Sci. Technol. A13 (1995) 1095–1099.
[8] A.V. Singh, R.M. Mehra, A. Yoshida, A. Wakahara, J. Appl. Phys. 95 (2004) 3640–3643.
[9] T. Yamamoto, T. Sakemi, K. Awai, S. Shirakata, Thin Solid Films 451–452 (2004) 439–442.
[10] K. Kakinuma, K. Kanda, H. Yamamura, J. Mater. Sci. 38 (2003) 7–11.
[11] S.D. Shannon, Acta Cryst. A32 (1976) 751–753.
[12] K. Kakinuma, K. Fueki, Phys. Rev. B. 56 (1997) 3494–3507.
[13] T. Minami, Ouyou Buturi 61 (1992) 1255–1258.
[14] M.W. Barsoum, Fundamentals of Ceramics, The McGraw-Hill Companies Inc., New York, 1997, pp. 58–61.